Supporting Information

Supramolecular Caging for Cytosolic Delivery of Anionic Probes

Héctor Fernández-Caro,[a] Irene Lostalé-Seijo,[a] Miguel Martínez-Calvo,[a] Jesús Mosquera,[b] José L. Mascareñas,*[a] Javier Montenegro*[a]

[a] Centro Singular de Investigación en Química Biolóxica e Materiais Moleculares (CIQUS) and Departamento de Química Orgánica, Universidade de Santiago de Compostela, 15782, Santiago de Compostela, Spain

[b] CIC biomaGUNE, Paseo Miramón 182, 20014, Donostia/San Sebastián, Spain

e-mail: joseluis.mascarenas@usc.es; javier.montenegro@usc.es

Table of Contents

1. Supporting Chemical Structures

A) ^{Tm}**A**

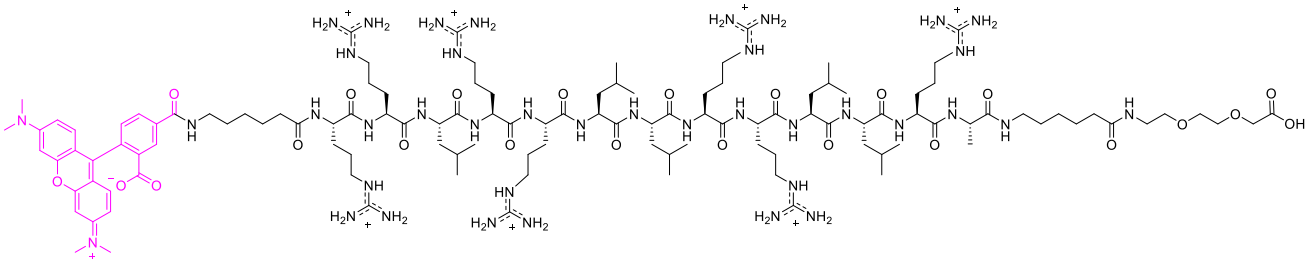

B) $^{Tm}\boldsymbol{R_8}$

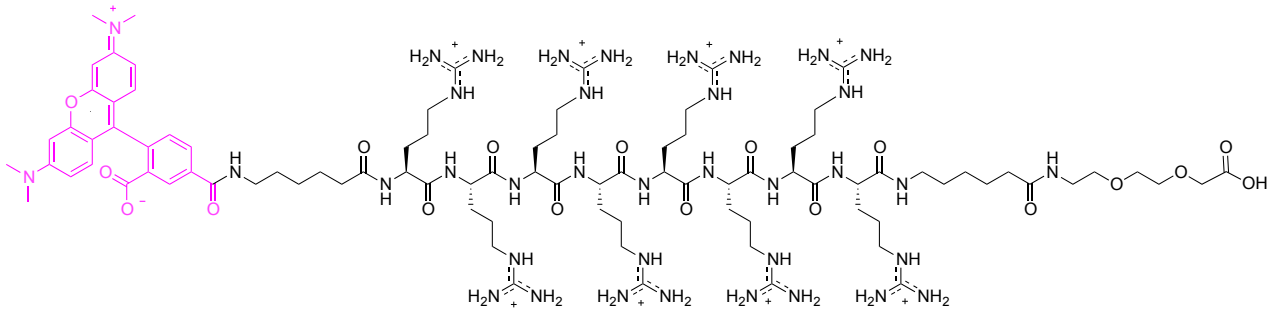

C) $^{Tm}\boldsymbol{R_4}$

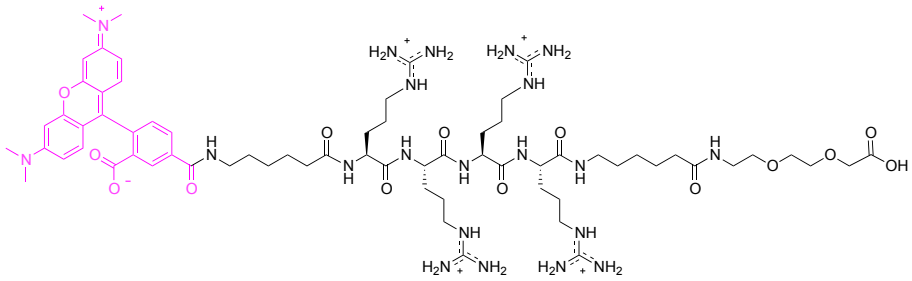

D) $^{Ac}\boldsymbol{R_4}$

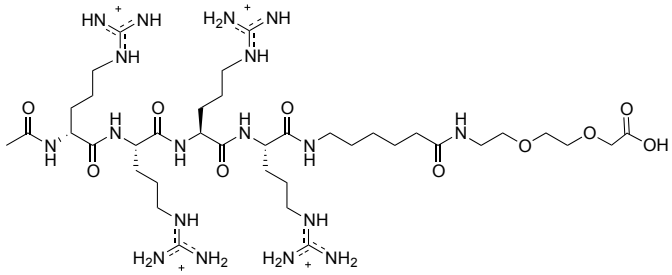

Figure S1. Chemical structures of the peptides A) ^{Tm}**A**, B) $^{Tm}\boldsymbol{R_8}$, C) $^{Tm}\boldsymbol{R_4}$, D) $^{Ac}\boldsymbol{R_4}$.

A) ^{Tm}**AC**

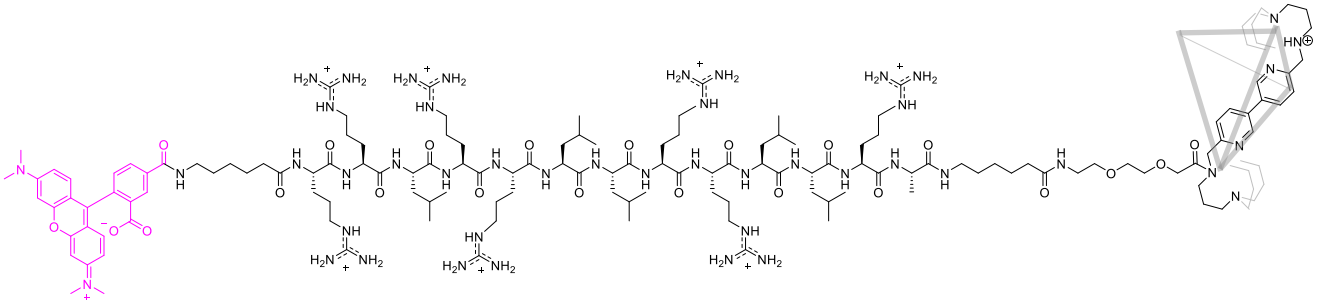

B) ^{Tm}***R*$_8$C**

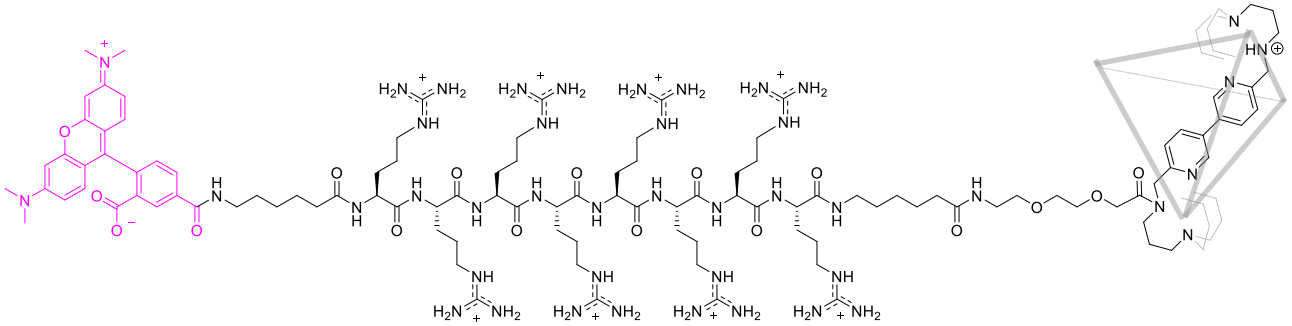

C) ^{Tm}***R*$_4$C**

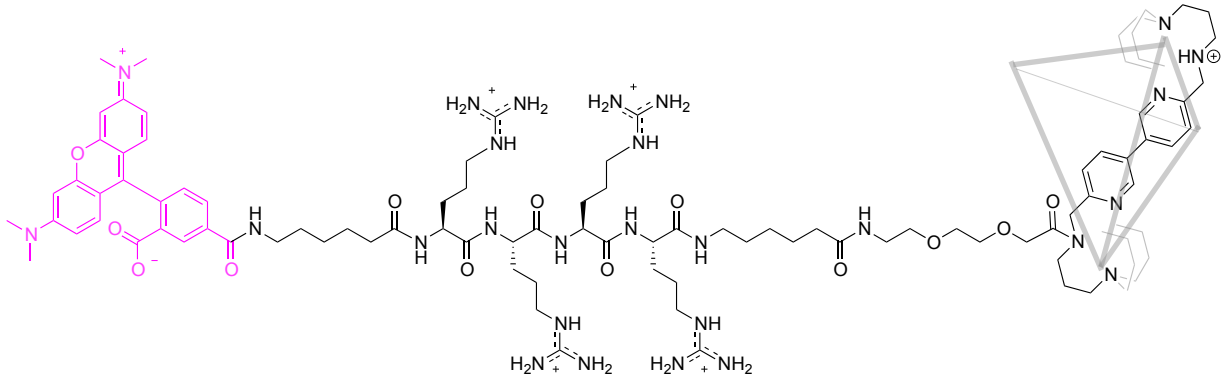

D) ^{Ac}***R*$_4$C**

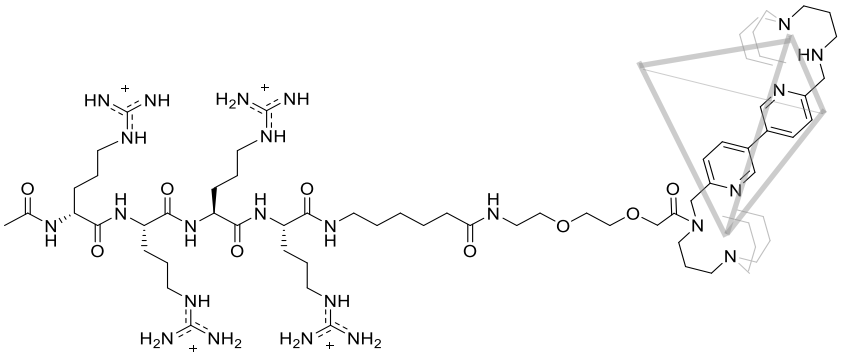

Figure S2. Chemical structures of the peptide-cage hybrids: A) ^{Tm}**AC**, B) ^{Tm}***R*$_8$C**, C) ^{Tm}***R*$_4$C**, D) ^{Ac}***R*$_4$C**.

2. Supporting figures

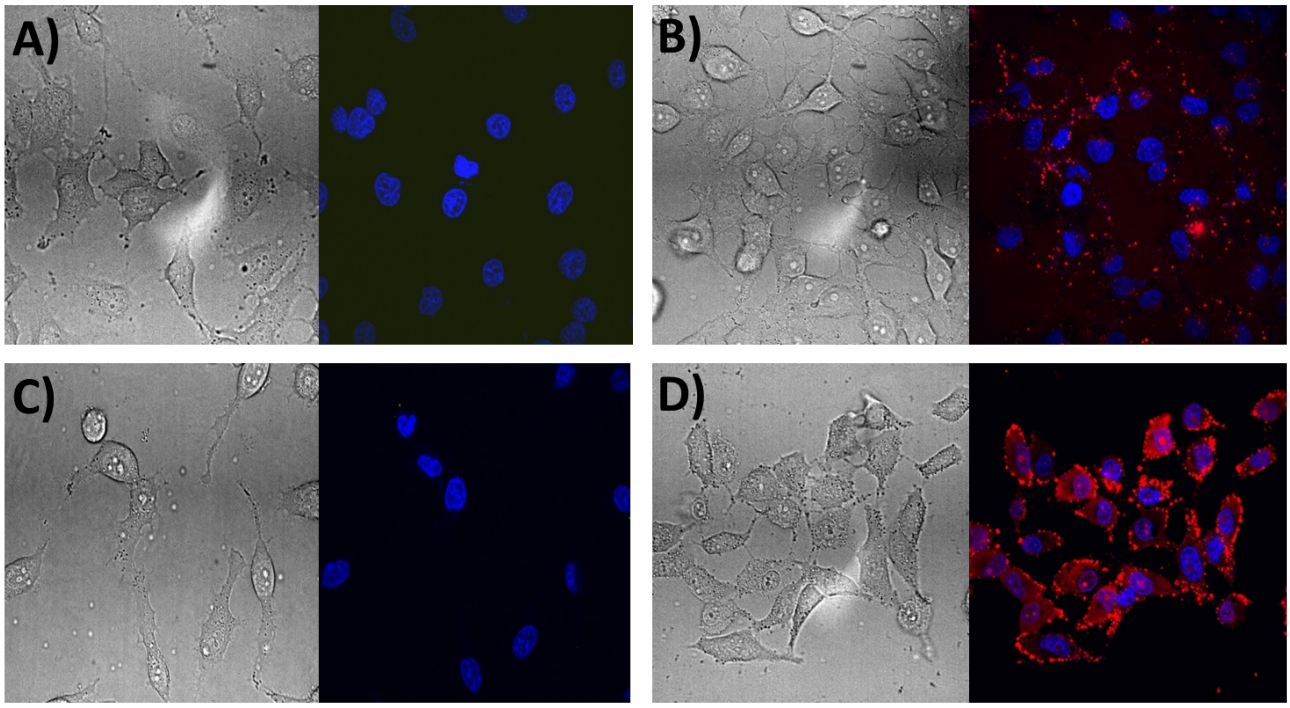

Figure S3. Control transport experiments in HeLa cells. Confocal micrographs of HeLa cells incubated with: A) Pyranine (5 µM) and only cage (5 µM). B) $^{Tm}\boldsymbol{R_4}$ (5 µM) and Pyranine (5 µM). C) Pyranine (5 µM). D) $^{Tm}\boldsymbol{R_4}$**C** (5 µM). DIC on the left and merge of fluorescence channels [Pyranine emission (green) + TAMRA emission (red) + Hoechst 33342 emission (blue)] on the right. HeLa cells were treated first with Hoechst 33342 for 30 min, washed (HKR buffer, 1x) and then incubated with the different controls in HKR buffer for 30 min at 37 ºC. The cells were finally washed (HKR buffer, 3x) and then observed under the confocal microscope.

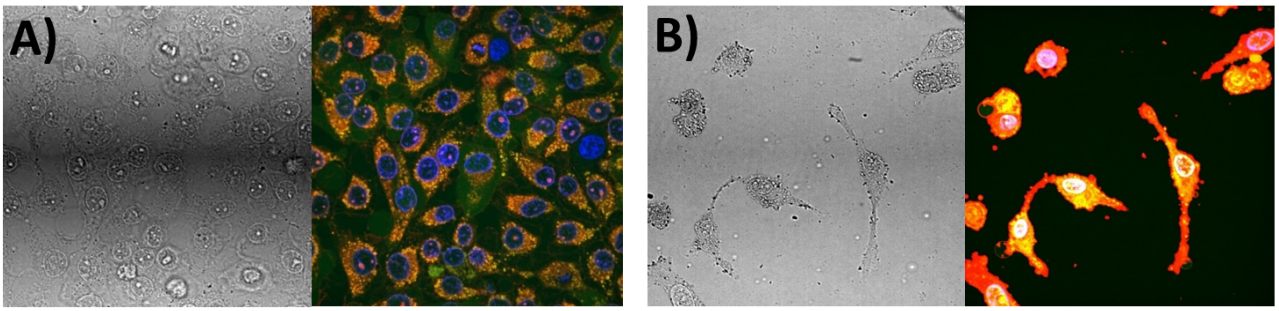

Figure S4. Transport experiments in HeLa cells with hybrids ^{Tm}AC and $^{Tm}\boldsymbol{R_8}$C. Confocal micrographs of HeLa cells incubated with: A) 5 µM of ^{Tm}**AC** and 5 µM Pyranine B) 5 µM of $^{Tm}\boldsymbol{R_8}$**C** and 5 µM Pyranine. DIC on the left and merge channels [Pyranine emission (green) + TAMRA emission (red) + Hoechst 33342 emission (blue)] on the right. HeLa cells were treated first with Hoechst 33342 for 30 min, washed (HKR buffer, 1x) and then incubated with the different mixtures in HKR buffer for 30 min at 37 ºC. The cells were finally washed (HKR buffer, 3x) and then observed under the confocal microscope. Toxicity was evident by the morphological alterations such as rounding or nuclear swelling (A and B) and the lower number of cells (B) observed in the differential interference contrast microscopy images (DIC).

· **1 Hour incubation time:**

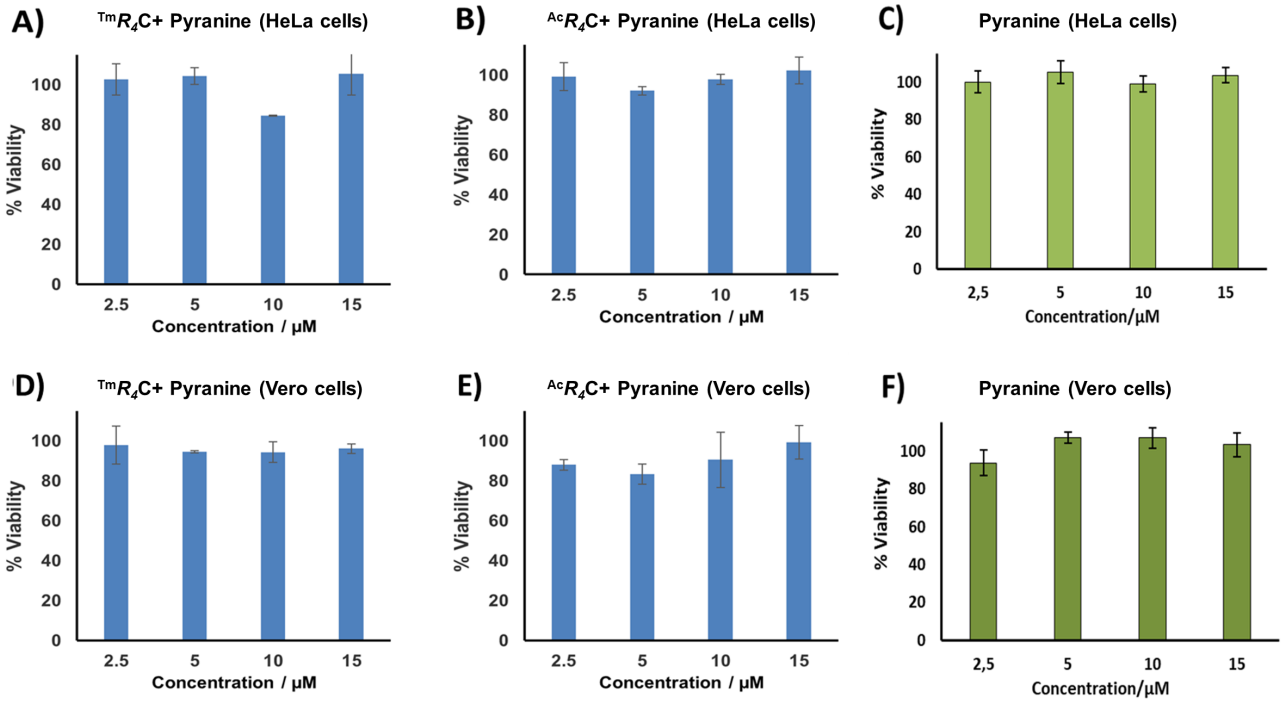

· **24 Hours incubation time:**

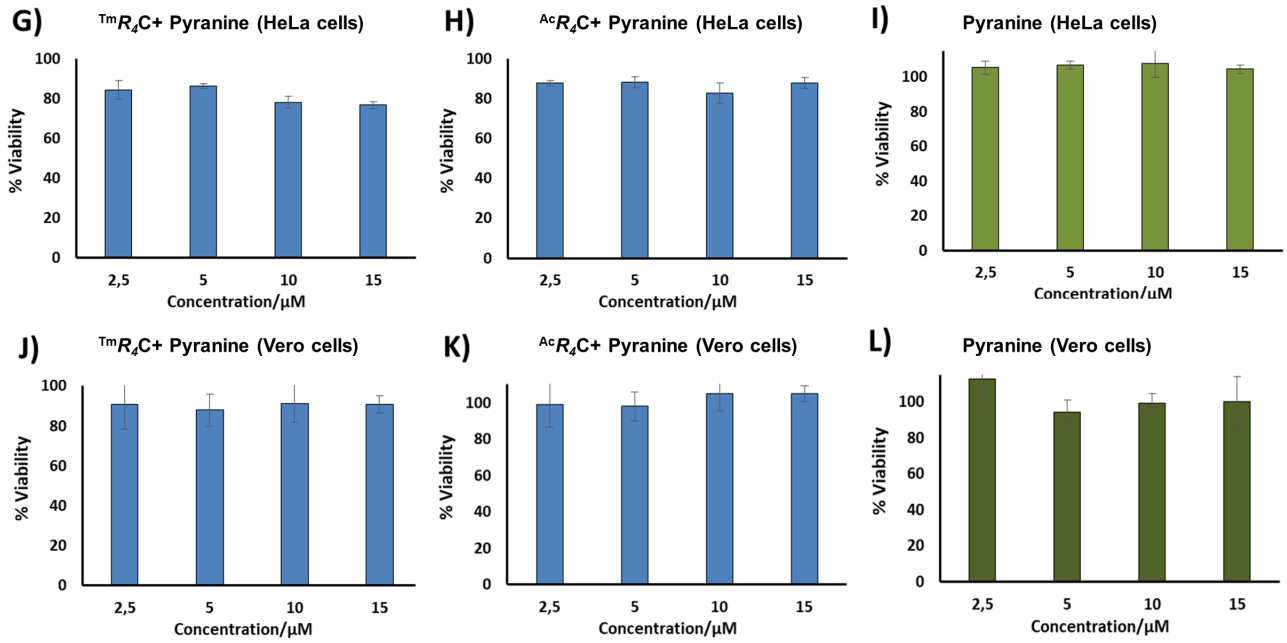

Figure S5. Viability assay in **HeLa** (A, B, C, G, H, I) and **Vero** cells (D, E, F, J, K, L) with the different peptides $^{Tm}\boldsymbol{R}_4\mathbf{C}$ (A, D, G, J), $^{Ac}\boldsymbol{R}_4\mathbf{C}$ (B, E, H, K) and **pyranine** (C, F, I, L) at different concentrations after 1 hour incubation time (A, B, C, D, E, F) and after 24 hours incubation time (G, H, I, J, K, L) at 37 ºC. Error bars represent standard deviation of four replicates.

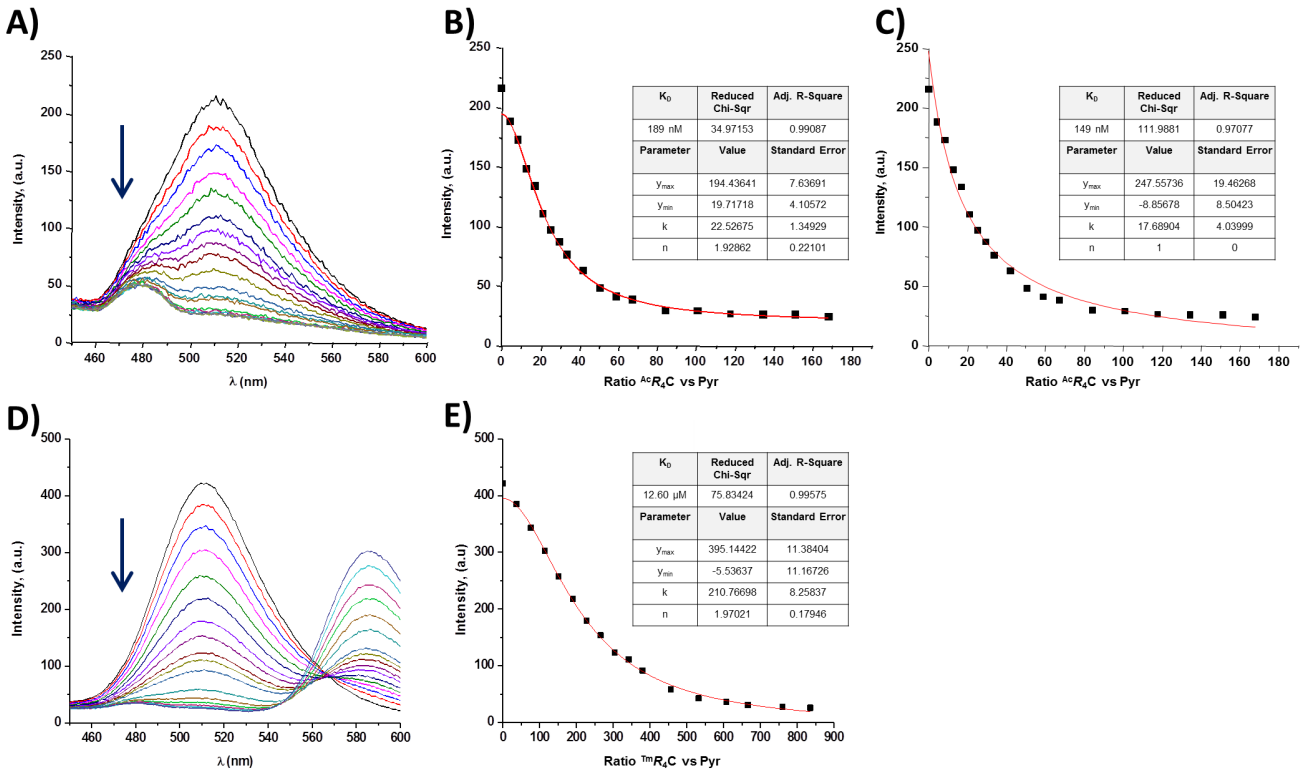

Figure S6. A) and D) Fluorescence titration of pyranine with the peptide/cage complexes $^{Ac}R_4C$ (A) and $^{Tm}R_4C$ (D) in phosphate buffer (pH 7). Arrow indicates the decrease of pyranine fluorescence with increasing amounts of peptide. The right peak in D corresponds to the TAMRA emission from $^{Tm}R_4C$. B), C) and E) 510 nm fluorescence emission and curve fit for the titration of pyranine with $^{Ac}R_4C$ (B, C) or with $^{Tm}R_4C$ (E) in phosphate buffer pH 7. The best fit to the data using nonlinear analysis with Origin 8.5 to the Hill 1 equation: K_D= 189 nM for $^{Ac}R_4C$ and K_D= 12.6 µM for $^{Tm}R_4C$. In C, fitting was done with a fixed value of n = 1, and K_D for $^{Ac}R_4C$ under these conditions was 149 nM. The small peak observed in A) at about 480 nm at the higher concentrations of peptide corresponds to the Raman scattering of water for an excitation wavelength of 415 nm.

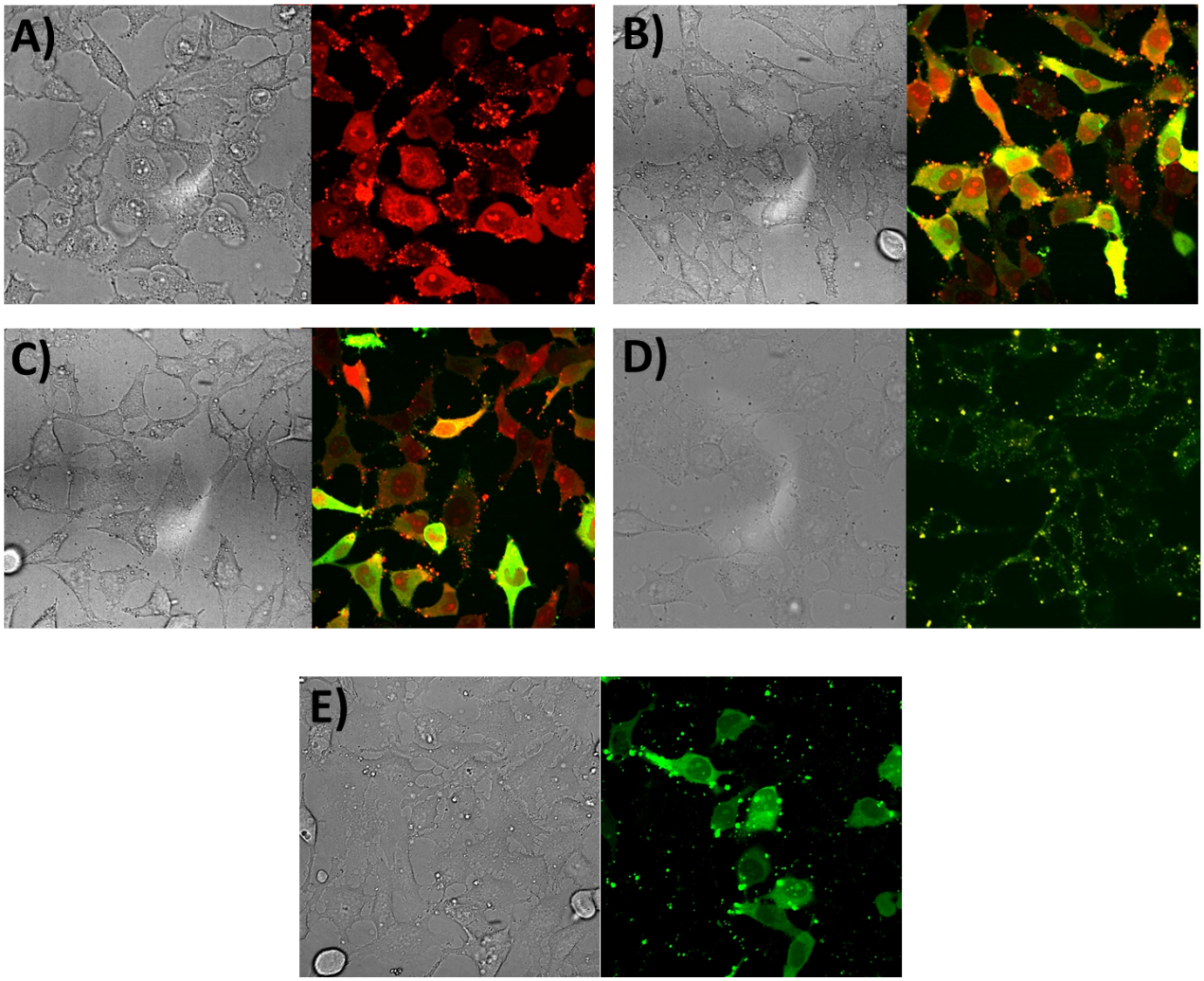

Figure S7. Dose-response transport experiments of pyranine in HeLa cells and pyranine delivery with the acetylated peptide. Confocal micrographs of HeLa cells incubated with: A) ^{Tm}***R*$_4$**C (5 μM), B) ^{Tm}***R*$_4$**C (5 μM) and Pyranine (2.5 μM), C) ***R*$_4$**C (5 μM) and Pyranine (5 μM), D) ^{Tm}***R*$_4$**C (5 μM) and Pyranine (10 μM). DIC on the left and merge channels [Pyranine emission (green) + Tm emission (red)] on the right. HeLa cells were incubated with the different components in HKR buffer for 30 min at 37 ºC. The cells were finally washed (HKR buffer, 3x) and then observed under the confocal microscope. E) The acetylated version, ^{Ac}***R*$_4$**C,** is also able to deliver pyranine in HeLa cells. Cells were incubated with ^{Ac}***R*$_4$**C (5 μM) and pyranine (5 μM; green) for 30 min at 37 ºC, washed (HKR buffer, 3x) and observed under the confocal microscope.

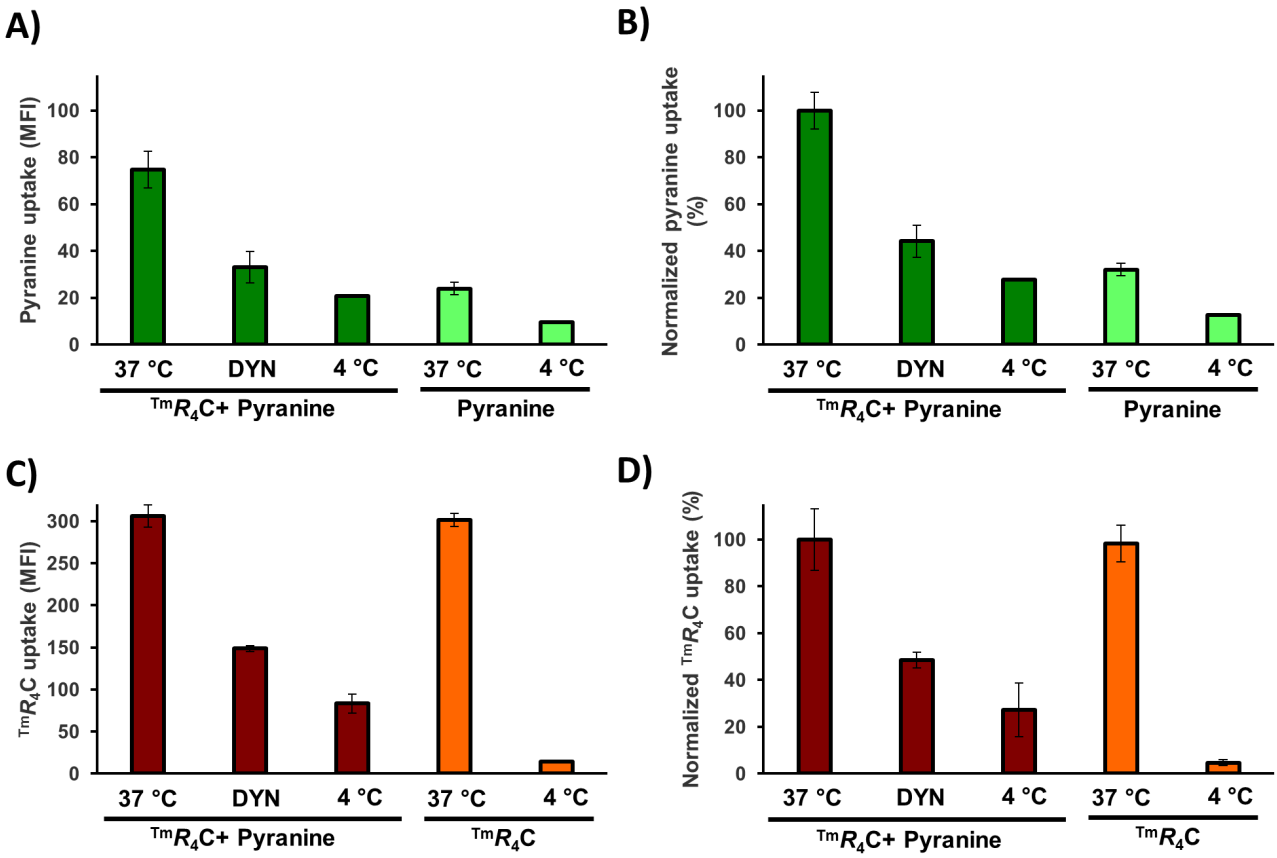

Figure S8. Quantification of the uptake of $^{Tm}R_4C$ (15 µM) and pyranine (15 µM) in Vero cells under different conditions: 37 ºC (control), DYN (dynasore, 80 µM) and 4 ºC. A) and C) median fluorescence intensity (MFI) corresponding to pyranine fluorescence (A) or $^{Tm}R_4C$ (C). B) and D) uptake normalized to the control of $^{Tm}R_4C$ with pyranine incubated at 37 ºC, corresponding to pyranine (B) or $^{Tm}R_4C$ (D). The last two bars in all charts indicate the uptake of pyranine (A, B) or $^{Tm}R_4C$ (C, D) when incubated alone. Error bars indicate SD of three replicates.

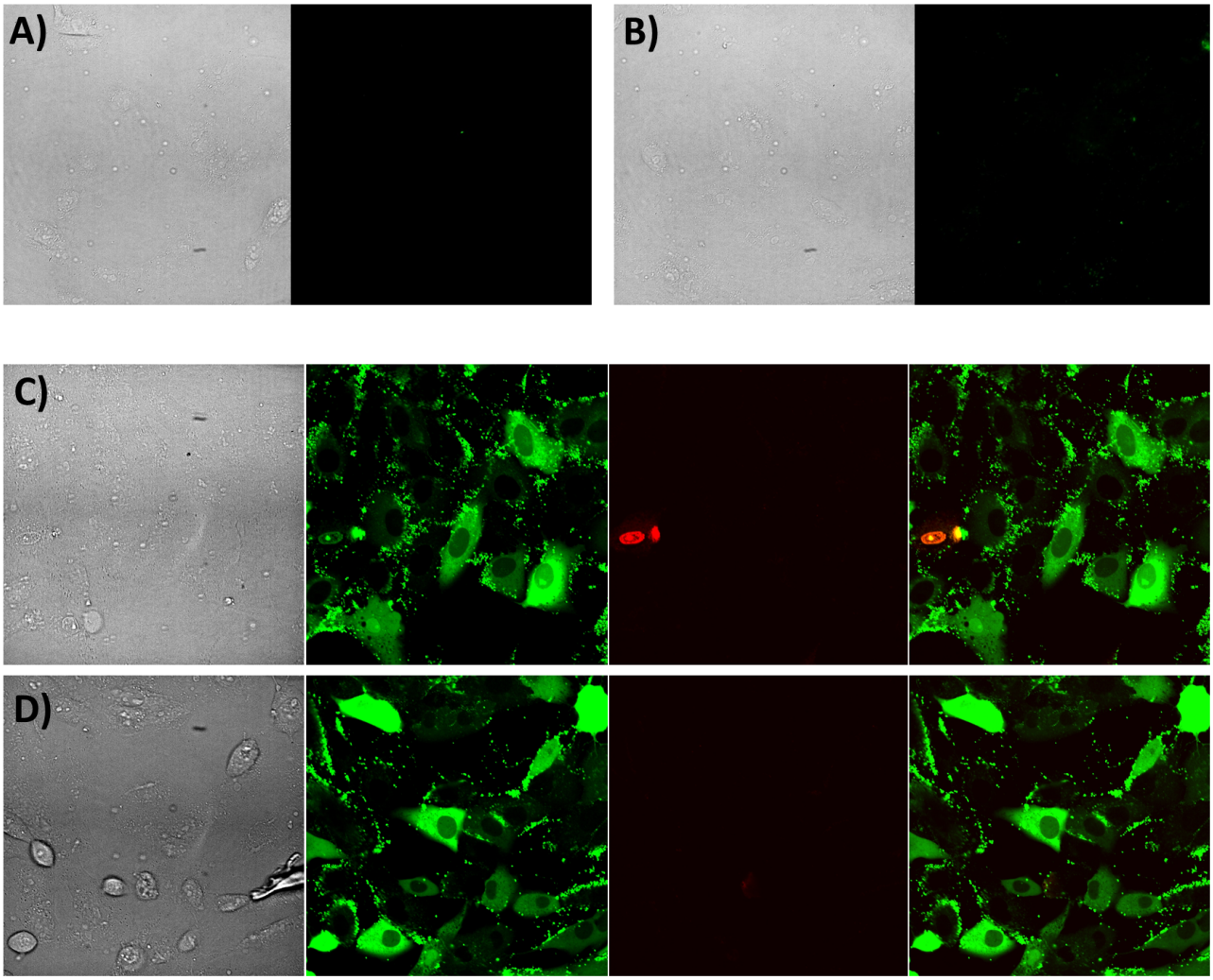

Figure S9. Internalization experiments in Vero cells. A) Vero cells incubated for 30 min with pyranine (10 μM, green) and only cage **C**. B) Vero cells incubated for 30 min with pyranine (10 μM, green) and $^{Ac}\boldsymbol{R_4}$**.** C) and D) Sequential addition of pyranine and $^{Ac}\boldsymbol{R_4}$**C** to Vero cells. Cells were incubated for ten minutes with pyranine before the dropwise addition of $^{Ac}\boldsymbol{R_4}$**C** to a final concentration of 10 μM and incubation for 30 minutes at 37 ^{o}C. Cells were stained with propidium iodide before imaging to detect membrane damage. Left panel: BF; second panel: pyranine (green); third panel: propidium iodide (red); right panel: merge of fluorescence channels. Images show internalization of pyranine and the aggregation of the pyranine/peptide complexes outside cells, but no membrane permeabilization of pyranine-loaded cells.

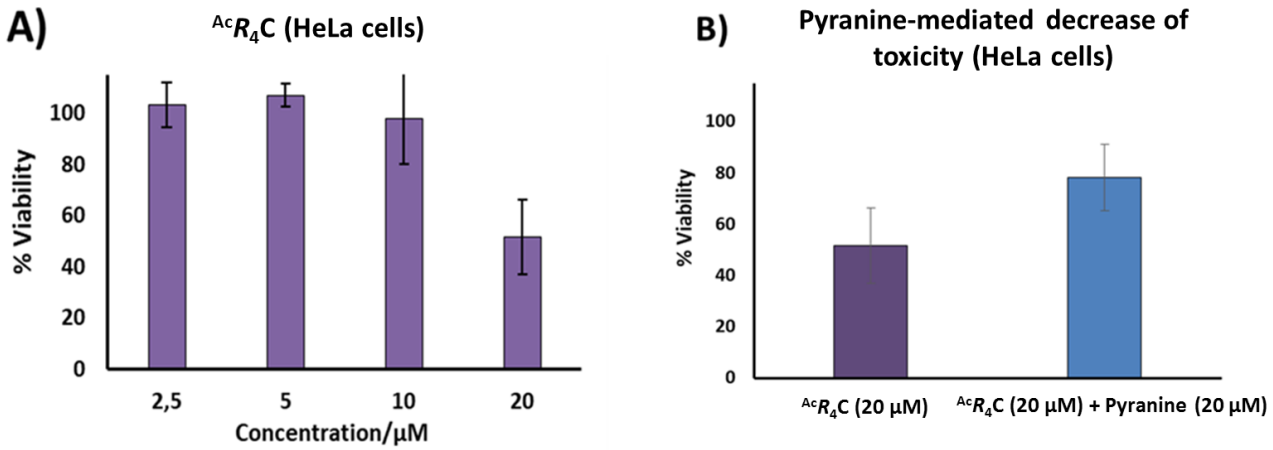

Figure S10. A) Viability assay in HeLa cells with $^{Ac}R_4C$ at different concentrations after 24 hours incubation time at 37 ºC. B) Viability comparison between $^{Ac}R_4C$ at 20 µM and $^{Ac}R_4C$ at 20 µM in presence of 20 µM of pyranine showing the decrease of toxicity produced by pyranine.

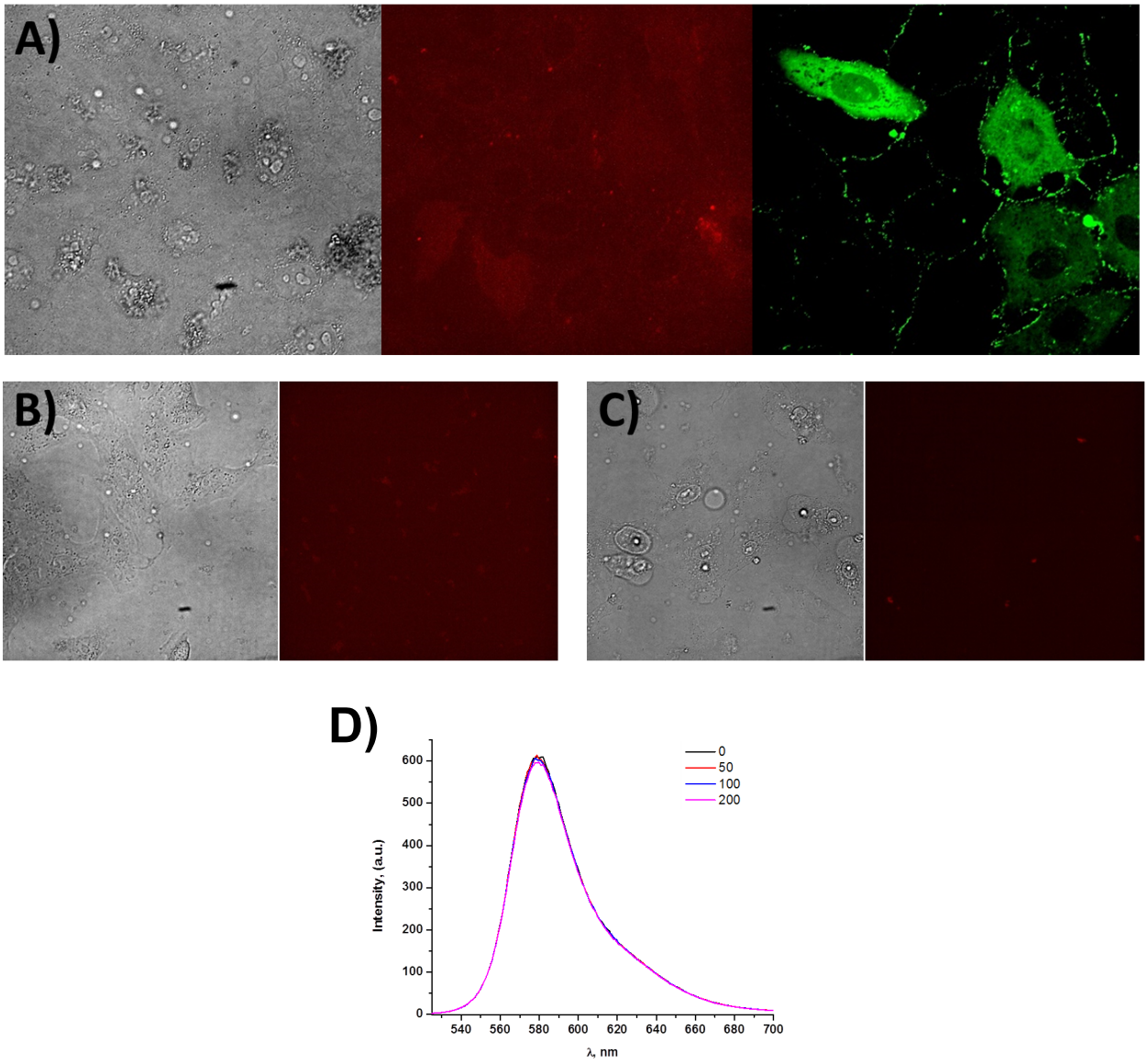

Figure S11. TAMRA competition experiments in Vero cells. Confocal micrographs of **Vero cells** incubated with: A) $^{Ac}\boldsymbol{R_4}$**C** (10 µM) combined with pyranine (20 µM, green) in the presence of TAMRA (20 µM, red) B) only TAMRA (20 µM, red channel). C) $^{Ac}\boldsymbol{R_4}$**C** (10 µM) in the presence of TAMRA (20 µM, red channel). Left panels correspond to DIC images. Vero cells were treated with the different conditions in HKR buffer for 30 min at 37 ºC. The cells were finally washed (HKR buffer, 3x) and then observed under the confocal microscope. D) Fluorescence spectra of the titration of 30 nM TAMRA fluorophore with increasing equivalents (50, 100 and 200) of $^{Ac}\boldsymbol{R_4}$**C**. No evidence of interaction could be found.

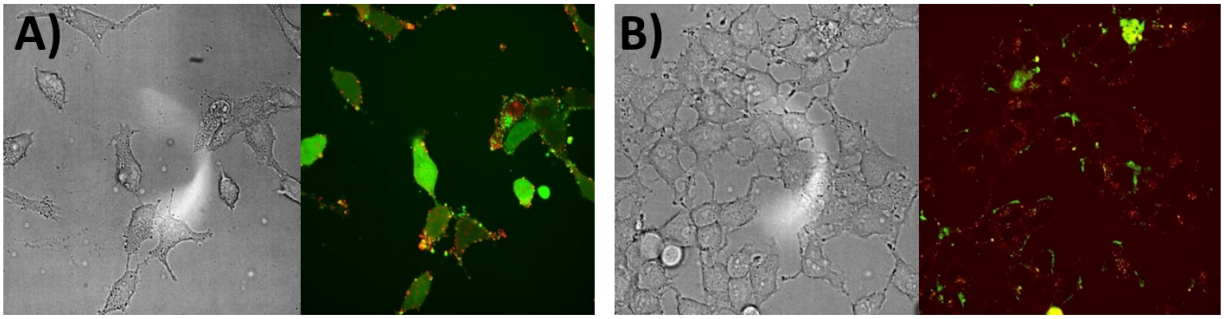

Figure S12. Transport experiments of Carboxyfluorescein (CF) in HeLa cells. Confocal micrographs of **HeLa cells** incubated with: A) $^{Tm}R_4C$ (5 μM) and **Carboxyfluorescein** (5 μM). B) $^{Tm}R_4$ (5 μM) and **Carboxyfluorescein** (5 μM). DIC on the left and merge channels [Carboxyfluorescein emission (green) + Tm emission (red)] on the right. HeLa cells were incubated with the different components in HKR buffer for 30 min at 37 ºC. The cells were finally washed (HKR buffer, 3x) and then observed under the confocal microscope.

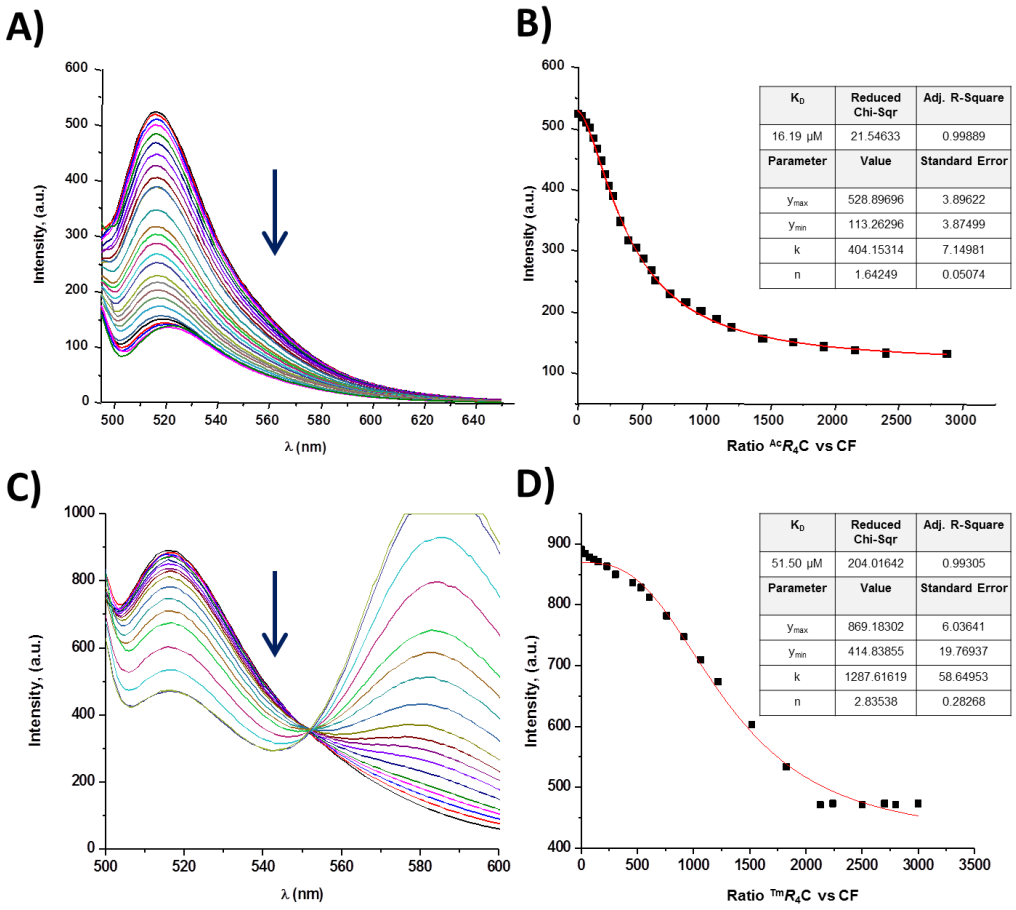

Figure S13. A) and C): Fluorescence spectra of the titration of CF with in $^{Ac}R_4C$ (A) or with $^{Tm}R_4C$ (C) in phosphate buffer (pH 7). Arrow indicates the decrease of CF fluorescence with increasing amounts of peptide. The right peak in C correspond to the TAMRA emission from $^{Tm}R_4C$. B) and D) 516 nm fluorescence emission and curve fit for the titration of **CF** with $^{Ac}R_4C$ (B) or with $^{Tm}R_4C$ in phosphate buffer (pH 7). The best fit to the data using nonlinear analysis with Origin 8.5 to the Hill 1 equation: K_D= 16.2 μM for $^{Ac}R_4C$ and K_D= 51.5 μM for $^{Tm}R_4C$.

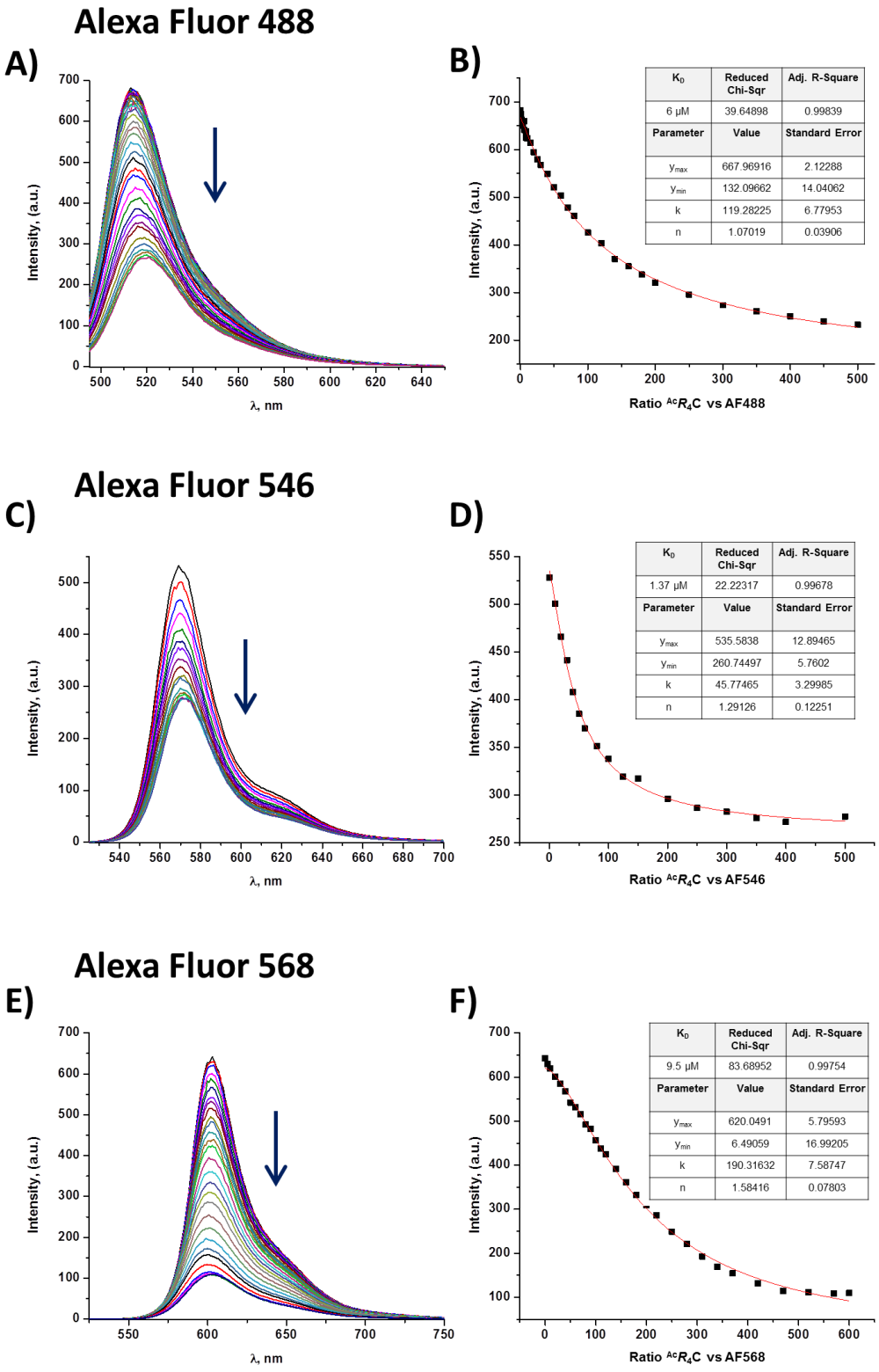

Figure S14. A), C) and E): Fluorescence spectra of the titration of Alexa Fluor dyes with $^{Ac}R_4C$. Arrows indicate the decrease of fluorophore emission with increasing amounts of $^{Ac}R_4C$. B), D) and F) Fluorescence emission at the maximum of each fluorophore (513 nm for Alexa Fluor 488, 570 nm for Alexa Fluor 546 and 603 nm for Alexa Fluor 568), and curve fit for the titration with $^{Ac}R_4C$ in phosphate buffer (pH 7). A), B): Alexa Fluor 488; C), D): Alexa Fluor 546; E), F): Alexa Fluor 568. The best fit to the data using nonlinear analysis with Origin 8.5 to the Hill 1 equation: K_D= 6 µM for Alexa Fluor 488, K_D= 1.37 µM for Alexa Fluor 546, and K_D= 9.5 µM for Alexa Fluor 568.

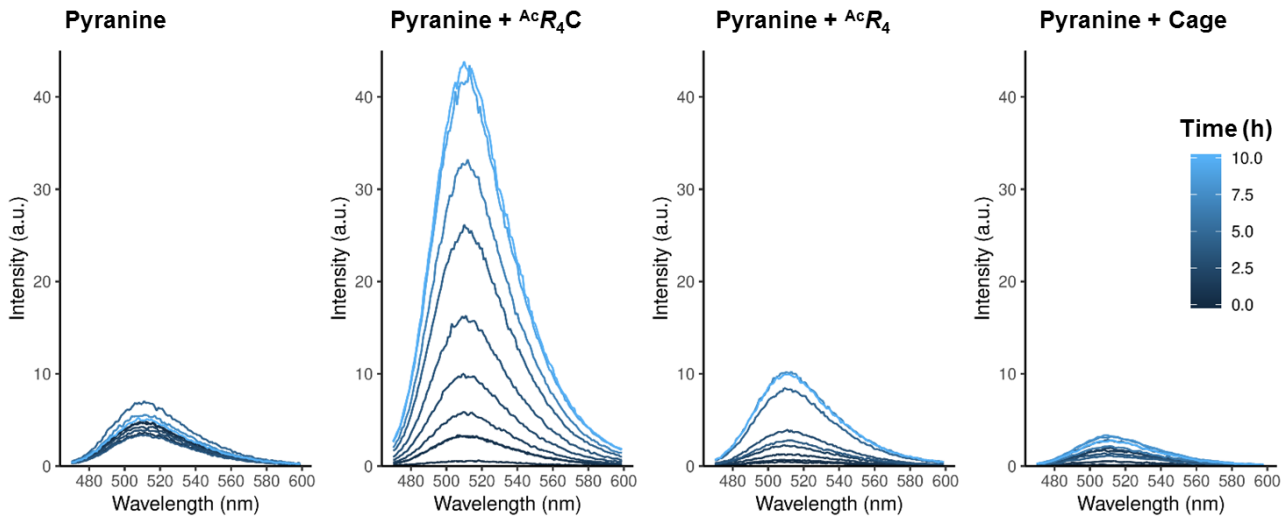

Figure S15. Pyranine fluorescence emission spectra of the aliquots taken from the U-Tube *trans* buffer at different times (10 mM $Na_mH_nPO_4$, 100 mM NaCl, pH 7.4). A) Pyranine alone (200 µM). B) Pyranine (200 µM) + $^{Ac}\boldsymbol{R_4}$C (80 µM) C) Pyranine (200 µM) + $^{Ac}\boldsymbol{R_4}$ (80 µM) D) Pyranine (200 µM) + Cage alone (80 µM).

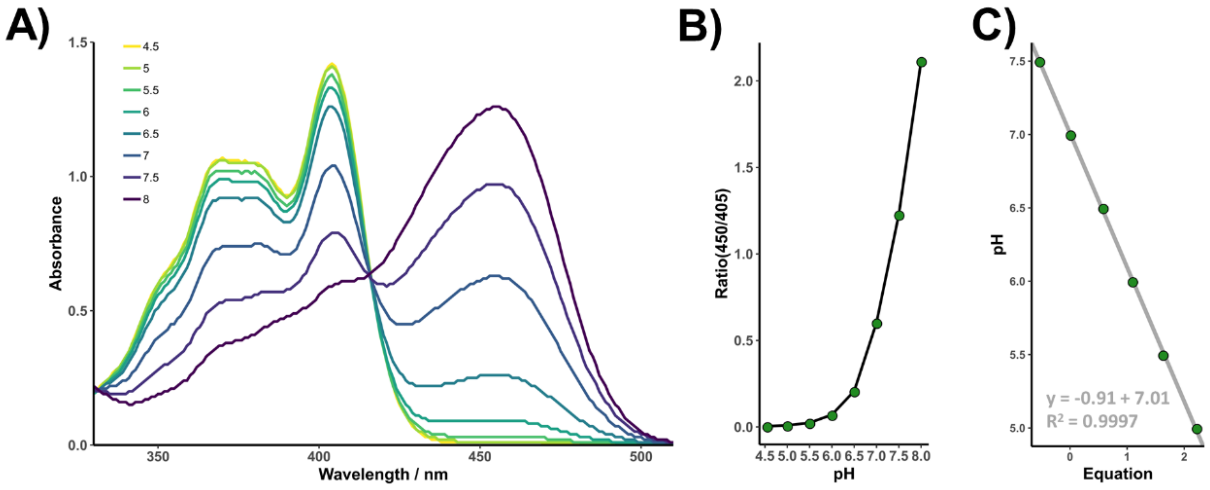

Figure S16. A) Absorption spectra of pyranine in buffers of different pH. B) Ratio of the absorbance at 450 and 405 nm plotted as a function of pH. C) Ratiometric method for determining the pK_a (see experimental section for details). pK_a = 7.01.

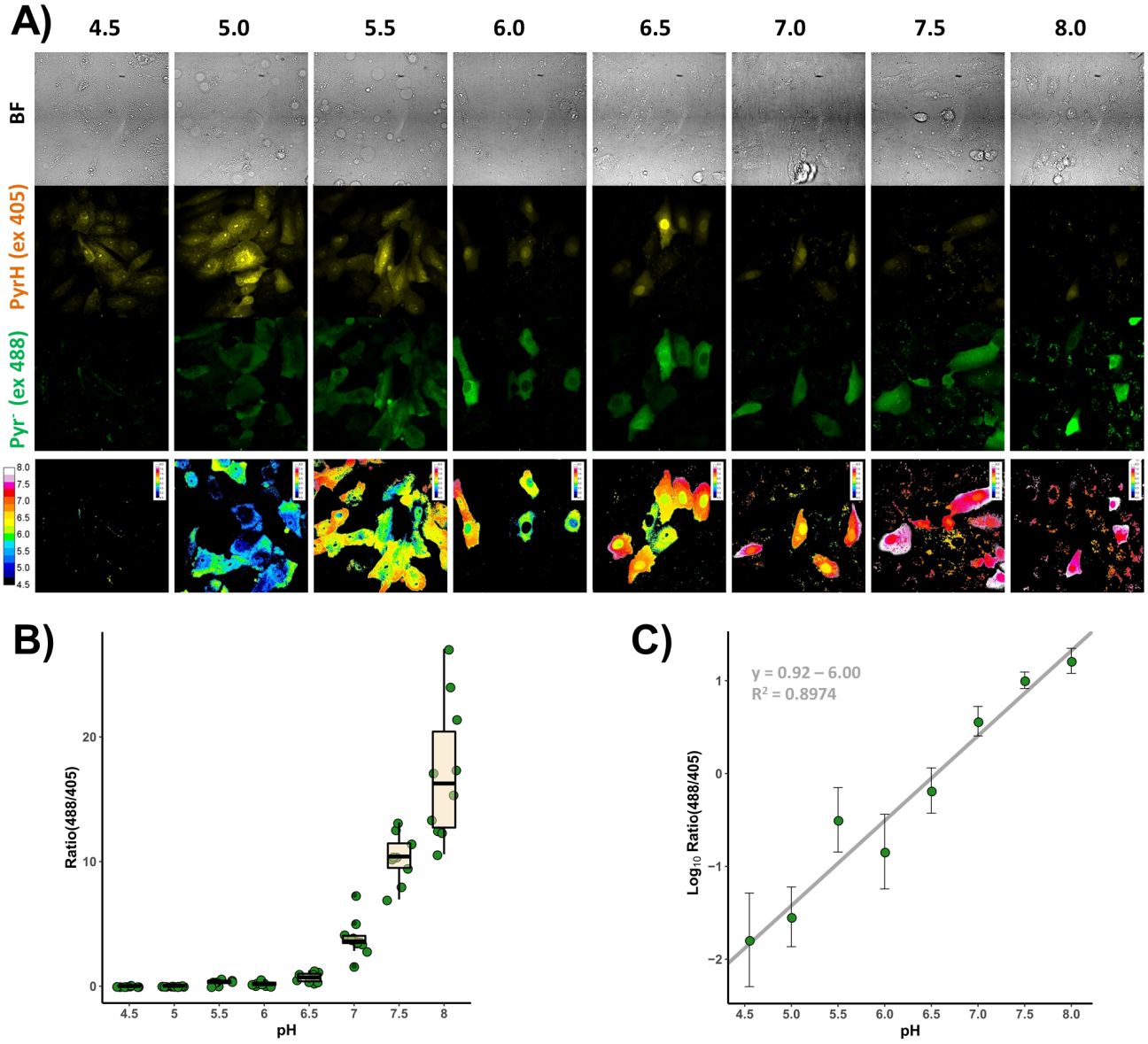

Figure S17. pH studies in Vero cells A) Ratiometric imaging after pH clamping with nigericin of Vero cells incubated with 10 µM pyranine and 10 µM $^{Tm}R_4$C. Top row (BF) shows bright field images. The second (PyrH) and third (Pyr^-) rows show the emission of pyranine after excitation at 405 nm or 488 nm, respectively. Finally, the bottom row shows the processed images. B) Mean ratio values were obtained for each field and plotted against pH. Box and whisker plot of each dataset, green points represent individual observations. C) Logarithmic conversion of the previous data and linear fit. Error bars indicate SD.

3. Materials and methods

Chemicals were purchased from Carbosynth, Iris Biotech, Sigma Aldrich, Alfa Aesar, Stream Chemicals and Novabiochem and used without further purification.

Commercially available 2-Chlorotrityl chloride resin, Fmoc-Ahx-OH, Fmoc-O2Oc-OH, Fmoc-*L*-Ala-OH, Fmoc-*L*-Leu-OH, Fmoc-*L*-Arg(pbf)-OH, triisopropylsilane (TIS), Disopropylethyl amine (DIEA), Nigericin and 8-Hydroxypyrene-1,3,6-trisulfonic acid trisodium salt (pyranine) were obtained from Sigma-Aldrich. MTT and MES (2-(N-morpholino)ethanesulfonic acid) were purchased from Alfa Aesar; 5(6)-Carboxyfluorescein (CF) and 5-Carboxytetramethyl rhodamine (TAMRA) were available from Carbosynth. L-α-phosphatidylglycerol (Egg, Chicken) (sodium salt) was purchased from Avanti Polar Lipids and *N*-HATU from Glentham life sciences. *N*-HBTU was obtained from Iris. Hoechst 33342 Trihydrochloride Trihydrate, Alexa Fluor dyes (488, 546 and 594) and Dulbecco's Modified Eagle's Medium (4500 mg/L glucose, L-glutamine, sodium pyruvate and sodium bicarbonate) were purchased in ThermoFisher. HEPES [4-(2-hydroxyethyl)-1-piperazineethanesulfonic acid)] was purchased from TCI Chemicals.

The solvents for organic synthesis were of reagent grade. Dry solvents were bought from Sigma-Aldrich. *N,N*-dimethylformamide and trifluoroacetic acid were purchased from Scharlau, dichloromethane from Panreac and acetonitrile from Merck. Water was deionized and purified on a Millipore Milli-Q Integral system.

The removal of solvents under reduced pressure was carried out on a rotary evaporator Büchi R-210 equipped with a thermostated bath B-491, a vacuum regulator V-850, and a vacuum pump V-700.

Purification of products was accomplished using reversed-phase high-performance liquid chromatography (RP-HPLC) using an Agilent Technologies 1160 Infinity using H_2O (+ 0.1% TFA) and CH_3CN (+ 0.1% TFA) as eluents and a Luna (C18)-Phenomenex column and on Jasco LC-4000 with an Agilent Eclipse XDB-C18 column.

High-performance liquid chromatography coupled with mass spectrometry (HPLC-MS) analyses were carried out on Agilent Technologies 1260 Infinity II associated with a 6120 Quadrupole LC-MS using an Agilent SB-C18 column or on DIONEX Ultimate 3000 U-HPLC$^+$ (Thermo Scientific) with an Acclaim RSLC 120-C18 column with *Solvent A*:*Solvent B* gradients between 5:95 (*Solvent A*: H_2O with 0.1% TFA; *Solvent B*: CH_3CN with 0.1% TFA).

Fluorescence measurements were performed using a Varian Cary Eclipse fluorometer and UV-Vis spectra were measured in an Agilent 8453 UV-Vis diode-array spectrophotometer or a Biochrom Libra S60 UV-vis spectrophotometer.

For taking confocal microscopy images a Dragonfly confocal spinning-disk system mounted on a Nikon Eclipse Ti-E equipped with an Andor Zyla 4.2 PLUS sCMOS digital camera was used.

The 3D reconstructions were obtained from the different individual confocal planes with Imaris bitplane 9.0.0 software.

A Tecan Infinite F200Pro microplate reader was used to measure directly in Costar cell culture 96-well plates UV-Vis absorbance for the MTT viability assays.

Flow cytometry was performed on a Guava easyCyte^{TM} cytometer. Data analysis was performed with InCyte software included in GuavaSoft 3.2 (Millipore).

The "U-tubes" were house made.

ABBREVIATIONS:

Ahx: 6-aminohexanoic acid; Arg: Arginine; calcd: calculated; CF: carboxyfluorescein; DMEM: Dulbecco's Modified Eagle Medium; DIEA: N,N-Diisopropylethylamine; DMF: N,N-Dimethylformamide; DYN: Dynasore; EYPG: Egg yolk phosphatidylglycerol; FBS: Fetal bovine serum; Fmoc: 9-Fluorenylmethoxycarbonyl; HEPES: 4-(2-hydroxyethyl)-1-piperazineethanesulfonic acid; HKR: HEPES-Krebs-Ringer buffer; Leu: Leucine; MES: 2-(N-morpholino)ethanesulfonic acid; MTT: (3-(4,5-dimethylthiazol-2-yl)-2,5-diphenyltetrazolium bromide) tetrazolium; N-HATU: N-[(Dimethylamino)-1H-1,2,3-triazolo[4,5-b]pyridine-1ylmethylene]-N-methylmethanaminium-hexafluorophosphate N-oxide; N-HBTU: N-[(1HBenzotriazol-1-yl)-(dimethylamino)methylene]-N-methylmethanaminium hexafluorophosphate N-oxide; Pbf: 2,2,4,6,7-Pentamethyldihydrobenzofuran-5-sulfonyl; SD: standard deviation; SPPS: solid phase peptide synthesis; TAMRA: 5-carboxytetramethyl rhodamine; TFA: trifluoroacetic acid; TIS: Triisopropylsilane; UV-vis: Ultraviolet-visible.

4. General protocol for synthetic procedures

Peptides ^{Tm}**A**, ^{Tm}***R*$_8$**, ^{Tm}***R*$_4$ and ^{Ac}***R*$_4$** were synthesized according to classic SPPS of peptides and further details are given below. The cage **C** (Fig. S18) was prepared and purified following the procedure reported in literature.[1,2]

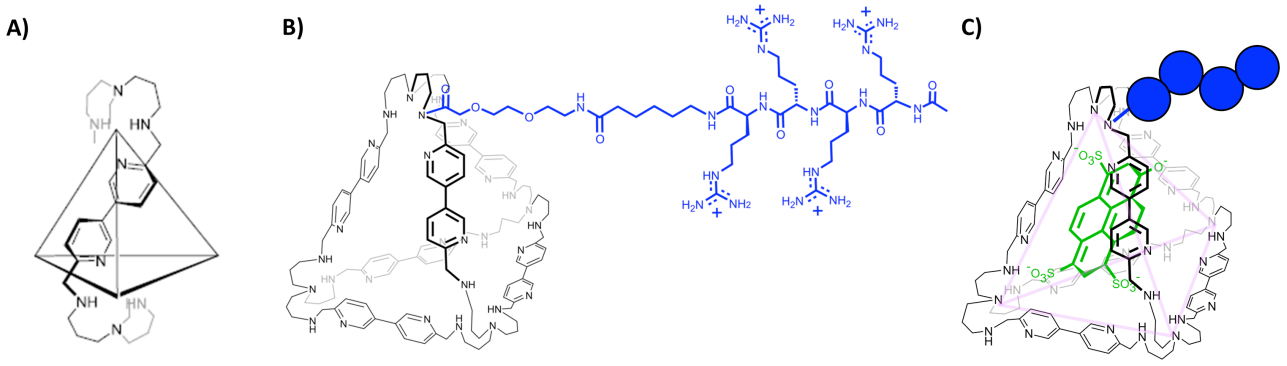

Figure S18. A) Cage **C** was synthesized according to the procedure reported in the literature.[1,2] For clarity, only one of the edges of the structure is shown. B) Structure of ^{Ac}***R*$_4$C** as a representative example of the attachment of the peptide to **C.** Only one peptide is attached to the cage. C) A representation of the peptide-cage hybrid with a pyranine molecule inside the cage.

4.1. Synthesis and characterization of the peptides ^{Tm}A, ^{Tm}*R*$_8$, ^{Tm}*R*$_4$ and ^{Ac}*R*$_4$

All peptides were synthesized by manual Fmoc solid-phase peptide synthesis on a 2-Chlorotrityl chloride resin (1.14 mmol/g). The first coupling was performed in CH_2Cl_2 using DIEA as base whereas for the following couplings HBTU as activator, DIEA as base, and DMF as solvent were used. The deprotection of the temporal Fmoc protecting group was performed by treating the resin with 20% piperidine in DMF. 5(6)-carboxytetramethylrhodamine (TAMRA) was coupled using 3 equivalents (0.15 mmol, 64.5 mg), 3 equivalents of HATU and 5 equivalents of DIEA 0.2 M in DMF for 60 min. Acetylation of the N-terminal group of ^{Ac}***R*$_4$** was performed by standard Fmoc removal conditions (20% piperidine in DMF) followed by treatment with a solution of acetic anhydride and 2,6- lutidine (1:1, 2 mL) for 30 min.

Cleavage/deprotection step was performed by treatment of the resin-bound peptide for 2 h with the following cleavage cocktail: 900 µL TFA, 50 µL CH_2Cl_2, 25 µL H_2O and 25 µL TIS (1 mL of cocktail/40 mg resin) and peptides were precipitated in Et_2O.

4.1.1. Synthesis and characterization of peptide ^{Tm}A

The synthesis of the peptide ^{Tm}**A** (TAMRA-Ahx-R-R-L-R-R-L-L-R-R-L-L-R-A-Ahx-O2Oc-OH) was performed following the above methodology. ^{Tm}**A** was obtained after RP-HPLC purification [Phenomenex Luna C18(2) 100A column, H_2O (0.1% TFA)/ CH_3CN (0.1% TFA) 95:5→5:95 (5→35 min)] with an overall yield of 12%. R_t 8.0 min [RP-HPLC Agilent SB-C18 column, H_2O (0.1% TFA)/ CH_3CN (0.1% TFA) 95:5→5:95 (0→12 min)] (Fig. S19). MS (ESI, H_2O) m/z: calcd for $C_{118}H_{204}N_{39}O_{23}$ $[M+5H]^{5+}$: 507.3, found: 507.5; calcd for $C_{118}H_{203}N_{39}O_{23}$ $[M+4H]^{4+}$: 633.9, found 634.0; calcd for $C_{120}H_{203}N_{39}O_{25}F_3$ $[M+3H+TFA]^{3+}$:

882.9, found: 883.0; calcd for $C_{122}H_{204}N_{39}O_{27}F_6$ $[M+3H+2TFA]^{3+}$: 920.9, found: 920.9; calcd for $C_{122}H_{203}N_{39}O_{27}F_6$ $[M+2H+2TFA]^{2+}$: 1380.8, found: 1380.7.

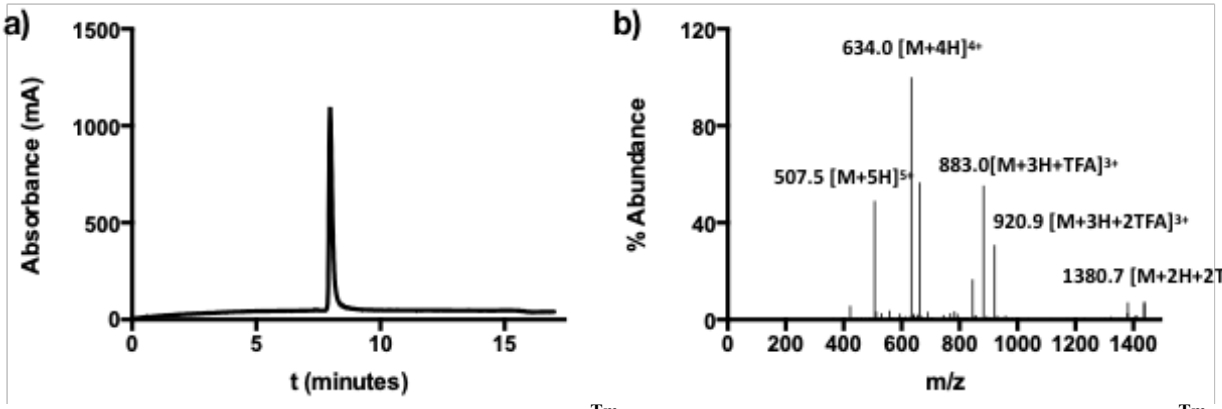

Figure S19. Representation of the HPLC-MS for ^{Tm}**A.** a) HPLC chromatogram (λ_{abs} = 550 nm) of ^{Tm}**A** and b) ESI-MS recorded at 8.0 min of ^{Tm}**A**.

4.1.2. Synthesis and characterization of peptide ^{Tm}***R*$_8$**

The synthesis of the peptide ^{Tm}***R*$_8$** (TAMRA-Ahx-R-R-R-R-R-R-R-R-Ahx-O2Oc-OH) was performed following the above methodology. ^{Tm}***R*$_8$** was obtained after RP-HPLC purification [Phenomenex Luna C18(2) 100A column, H_2O (0.1% TFA)/ CH_3CN (0.1% TFA) 95:5→5:95 (5→35 min)] with an overall yield of 12%. R_t 10.9 min [RP-HPLC Agilent SB-C18 column, H_2O (0.1% TFA)/ CH_3CN (0.1% TFA) 75:5→5:75 (0→21 min)] (Fig. S20). MS (ESI, H_2O) m/z: calcd for $C_{91}H_{156}N_{37}O_{18}$ $[M+5H]^{5+}$: 411.0, found: 411.3; calcd for $C_{93}H_{156}N_{37}O_{20}F_3$ $[M+4H+TFA]^{4+}$: 542.1, found: 542.3; calcd for $C_{93}H_{155}N_{37}O_{20}F_3$ $[M+3H+TFA]^{3+}$: 722.4, found: 722.9; calcd for $C_{95}H_{156}N_{37}O_{22}F_6$ $[M+3H+2TFA]^{3+}$: 760.4, found: 760.6; calcd for $C_{97}H_{156}N_{37}O_{24}F_9$ $[M+2H+3TFA]^{2+}$: 1197.1, found: 1197.6.

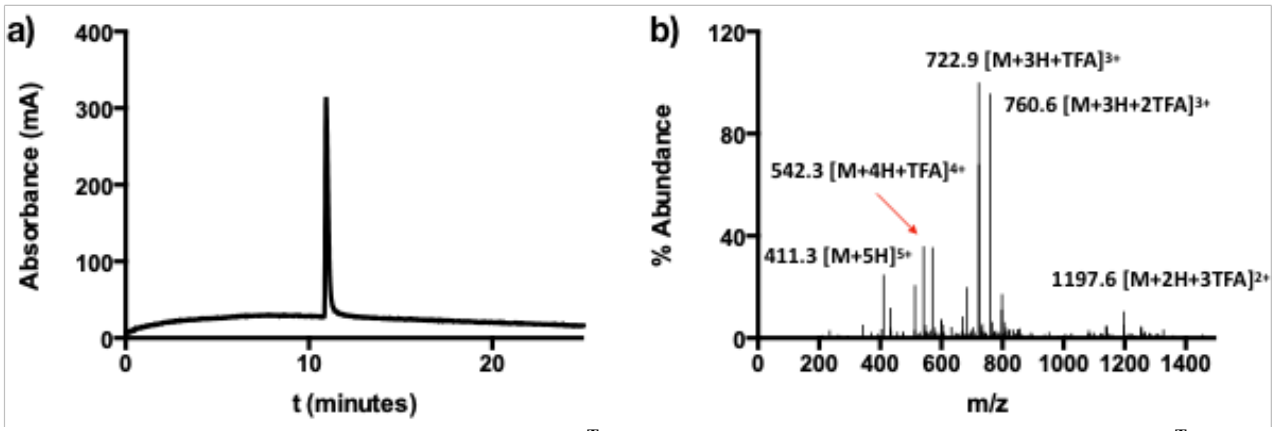

Figure S20. Representation of the HPLC-MS for ^{Tm}***R*$_8$.** a) HPLC chromatogram (λ_{obs} = 550 nm) of ^{Tm}***R*$_8$** and b) ESI-MS recorded at 10.9 min of ^{Tm}***R*$_8$**.

4.1.3. Synthesis and characterization of peptide $^{Tm}R_4$

The synthesis of the peptide $^{Tm}R_4$ (TAMRA-Ahx-R-R-R-R-Ahx-O2Oc-OH) was performed following the above methodology. $^{Tm}R_4$ was obtained after RP-HPLC purification [Phenomenex Luna C18(2) 100A column, H_2O (0.1% TFA)/ CH_3CN (0.1% TFA) 95:5→5:95 (5→35 min)] with an overall yield of 12%. R_t 11.1 min [RP-HPLC Agilent SB-C18 column, H_2O (0.1% TFA)/ CH_3CN (0.1% TFA) 75:5→5:75 (0→21 min)] (Fig. S21). MS (ESI, H_2O) m/z: calcd for $C_{67}H_{107}N_{21}O_{14}$ $[M+4H]^{4+}$: 357.5, found: 357.8; calcd for $C_{67}H_{106}N_{21}O_{14}$ $[M+3H]^{3+}$: 476.3, found: 476.5; calcd for $C_{67}H_{105}N_{21}O_{14}$ $[M+2H]^{2+}$: 713.9, found: 714.0.

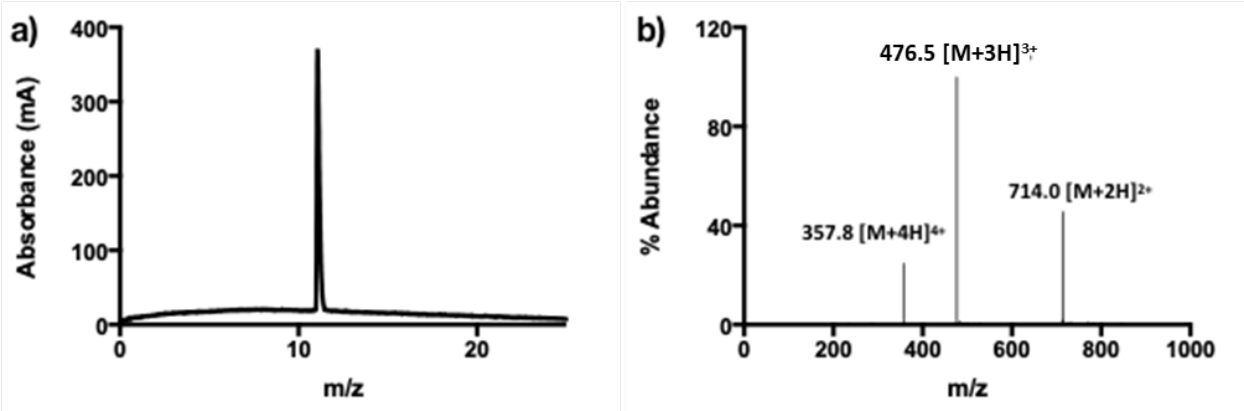

Figure S21. Representation of the HPLC-MS for $^{Tm}R_4$. a) HPLC chromatogram (λ_{obs} = 550 nm) of $^{Tm}R_4$ and b) ESI-MS recorded at 11.1 min of $^{Tm}R_4$.

4.1.4. Synthesis and characterization of peptide $^{Ac}R_4$

The synthesis of the peptide $^{Ac}R_4$ (Ac-R-R-R-R-Ahx-O2Oc-OH) was performed following the above methodology. $^{Ac}R_4$ was obtained after RP-HPLC purification [Phenomenex Luna C18(2) 100A column, H_2O (0.1% TFA)/ CH_3CN (0.1% TFA) 95:5→5:95 (0→5 min)] with an overall yield of 12%. R_t 2.9 min [RP-HPLC Agilent SB-C18 column, H_2O (0.1% TFA)/ CH_3CN (0.1% TFA) 95:5→5:95 (0→5 min)] (Fig. S22). MS (ESI, H_2O) m/z: calcd for $C_{38}H_{77}N_{18}O_{10}$ $[M+3H]^{3+}$: 315.2, found: 315.3; calcd for $C_{38}H_{76}N_{18}O_{10}$ $[M+2H]^{2+}$: 472.3, found: 472.4; calcd for $C_{38}H_{75}N_{18}O_{10}$ $[M+H]^{+}$: 943.6, found: 943.6; calcd for $C_{40}H_{77}N_{18}O_{12}F_3$ $[M+2H+TFA]^{2+}$: 529.3, found: 529.4.

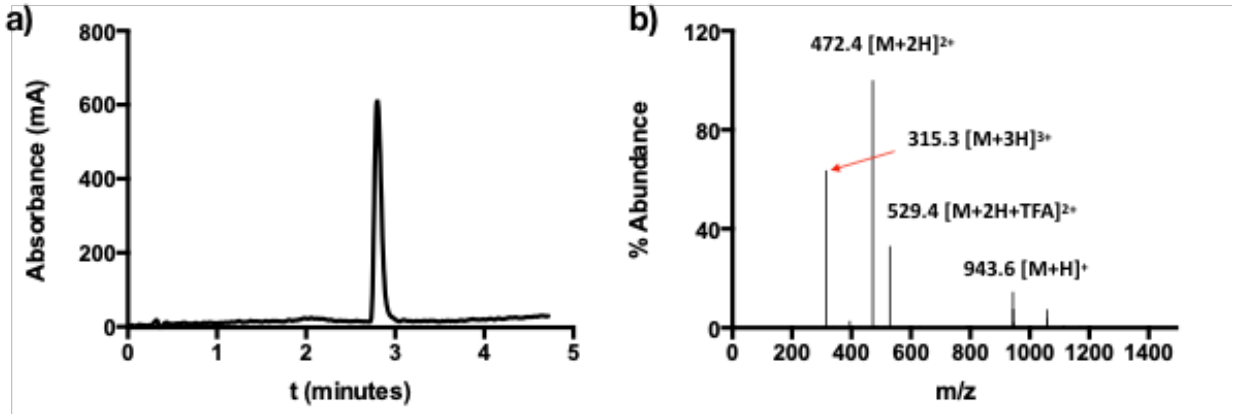

Figure S22. Representation of the HPLC-MS for $^{Ac}\boldsymbol{R_4}$ a) HPLC chromatogram (λ_{obs} = 222 nm) of $^{Ac}\boldsymbol{R_4}$ and b) ESI-MS recorded at 2.9 min of $^{Ac}\boldsymbol{R_4}$.

4.2. Synthesis and characterization of peptides ^{Tm}AC, $^{Tm}\boldsymbol{R_8}$C, $^{Tm}\boldsymbol{R_4}$C and $^{Ac}\boldsymbol{R_4}$C

For the synthesis of the supramolecular carriers the ^{Tm}**A**, $^{Tm}\boldsymbol{R_8}$, $^{Tm}\boldsymbol{R_4}$ and $^{Ac}\boldsymbol{R_4}$ peptides were solved in DMF (0.1 mM, 100 µL) before HATU (1 equiv) and DIEA (10 equiv) were added to the solution. This solution was added to a 0.1 mM solution of the cage **C**, adding 1 equiv of peptide to 1 equiv of **C**, and the reaction mixture was left stirring overnight.

4.2.1. Synthesis and characterization of peptide ^{Tm}AC

^{Tm}**A** was solved in 100 µL of DMF (10 mg, 0.004 mM) before HATU (6 mg, 0.016 mmol, 4 equiv) and DIEA (6.91 µL, 0.040 mmol, 10 equiv) were added to the solution of the cage **C** in 164 µL of DMF (7.3 mg, 0.004 mmol, 1 equiv). The reaction was left stirring overnight and the resulting reaction mixture was purified by RP-HPLC [Phenomenex Luna C18(2) 100A column, H_2O (0.1% TFA)/ CH_3CN (0.1% TFA) 85:15→55:45 (30 min)]. ^{Tm}**AC** was obtained after sample lyophilization as a purple solid (2 mg, 12 %). R_t 18.7 min (Fig. S23). MS (ESI, H_2O) m/z: calcd for $C_{234}H_{356}N_{67}O_{32}F_{12}$ $[M+7H+4TFA+2H_2O]^{7+}$: 692.4, found: 690.9 $[M+7H+4TFA+2H_2O]^{+7}$; calcd for $C_{230}H_{356}N_{67}O_{29}F_6$ $[M+7H+2TFA+3H_2O]^{7+}$:662.4, found: 662.4.

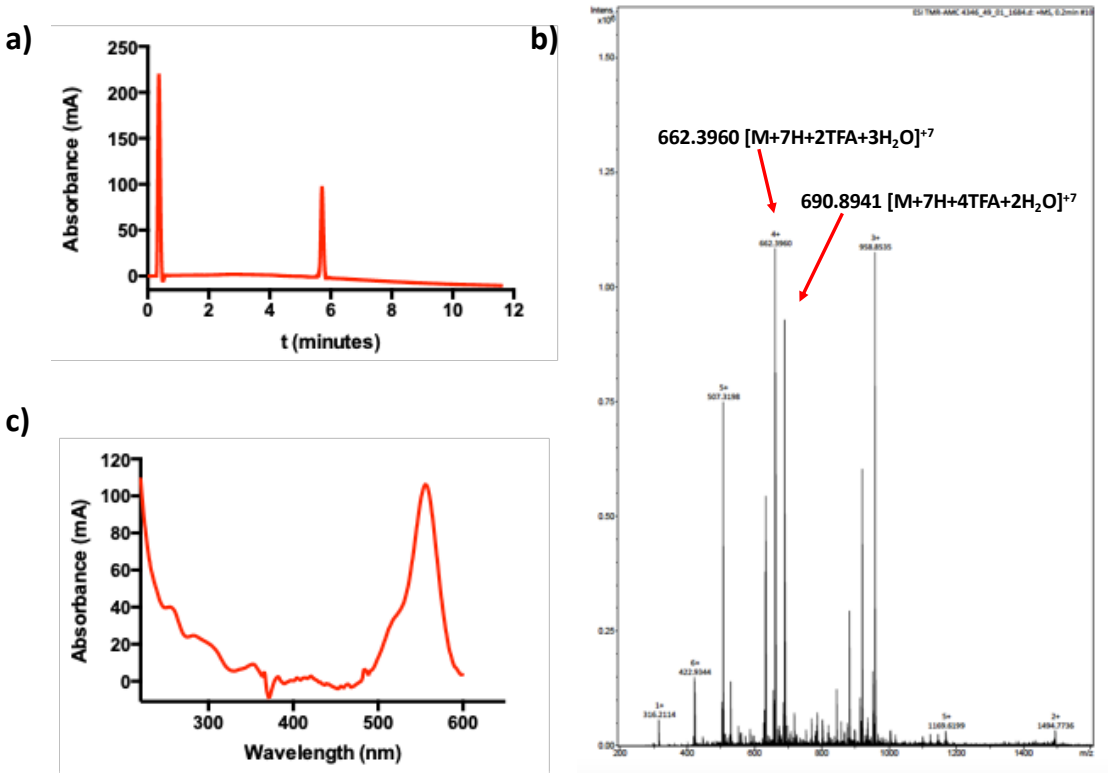

Figure S23. Representation of the HPLC-MS for ^{Tm}**AC.** a) HPLC chromatogram (λ_{obs} = 550 nm) of ^{Tm}**AC**and b) ESI-MS recorded at 5.73 min of ^{Tm}**AC**. c) UV-Vis spectrum at 5.73 minutes corresponding to ^{Tm}**AC.**

4.2.2. Synthesis and characterization of peptide $^{Tm}R_8C$

$^{Tm}R_8$ was solved in 100 µL of DMF (10 mg, 0.005 mM) before HATU (7.4 mg, 0.019 mmol, 4 equiv) and DIEA (8.5 µL, 0.05 mmol, 10 equiv) were added to the solution of the cage **C** in 225 µL of DMF (9.0 mg, 0.005 mmol, 1 equiv). The reaction was left stirring overnight and the resulting reaction mixture was purified by RP-HPLC. $^{Tm}R_8C$ was obtained after RP-HPLC purification [Phenomenex Luna C18(2) 100A column, H_2O (0.1% TFA)/ CH_3CN (0.1% TFA) 85:15→55:45 (30 min)] with an overall yield of 13% (2.5 mg). R_t 14.3 min (Fig. S24). MS (ESI, H_2O) m/z: calcd for $C_{201}H_{310}N_{65}O_{22}F_3$ $[M+10H+TFA+3H_2O]^{10+}$: 404.5, found: 404.0 $[M+10H+TFA+3H_2O]^{+10}$; calcd for $C_{201}H_{308}N_{65}O_{22}F_3$ $[M+8H+TFA+3H_2O]^{8+}$: 505.4, found: 504.8; calcd for $C_{201}H_{306}N_{65}O_{22}F_3$ $[M+6H+TFA+3H_2O]^{6+}$: 673.6, found: 672.7; calcd for $C_{203}H_{300}N_{65}O_{21}F_6Na$ $[M+5H+2TFA+Na]^{5+}$: 824.7, found: 824.7.

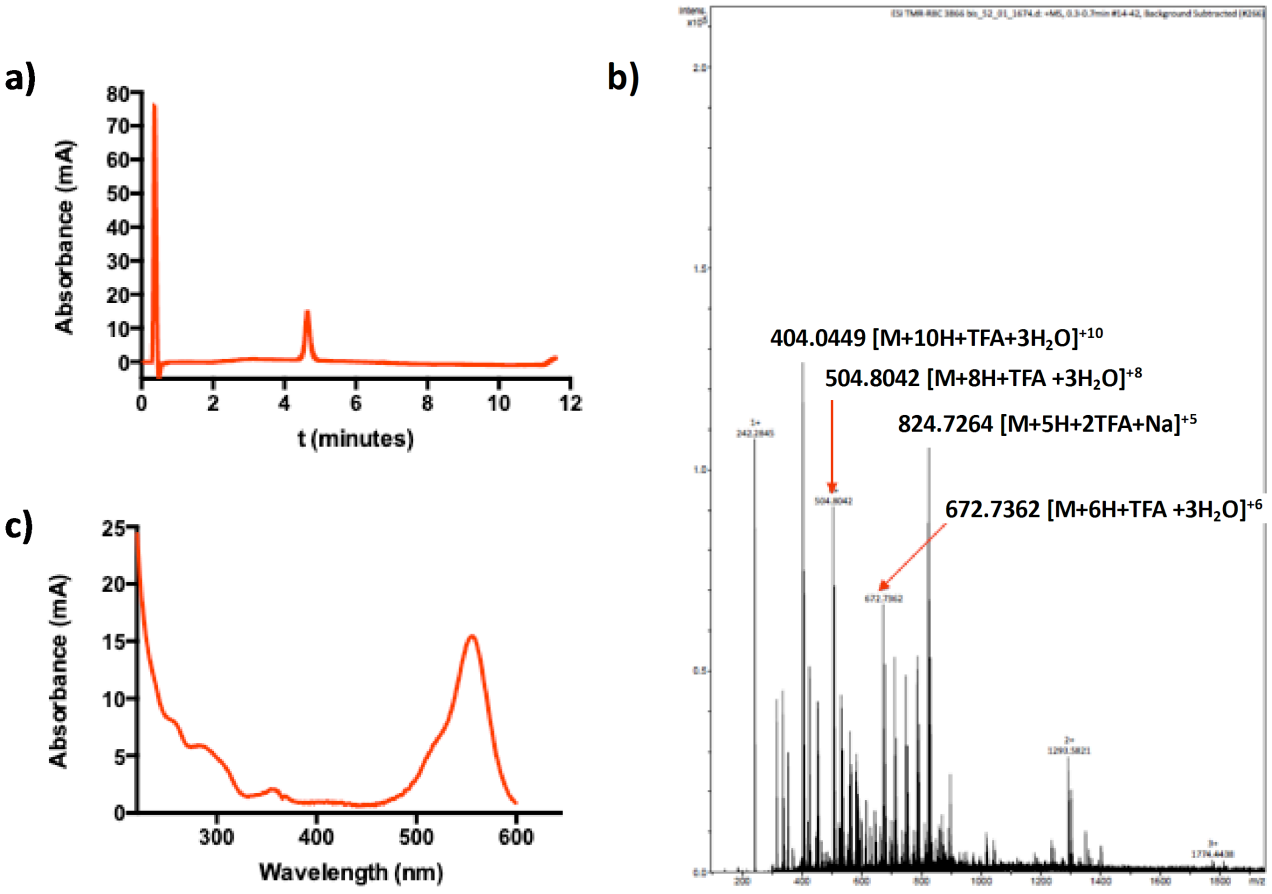

Figure S24. Representation of the HPLC-MS for $^{Tm}R_8C$ a) HPLC chromatogram (λ_{obs} = 550 nm) of $^{Tm}R_8C$ and b) ESI-MS recorded at 4.65 min of $^{Tm}R_8C$. c) UV-Vis spectrum at 4.65 minutes corresponding to $^{Tm}R_8C$.

4.2.3. Synthesis and characterization of peptide $^{Tm}R_4C$

$^{Tm}R_4$ was solved in 100 µL of DMF (12.9 mg, 0.007 mM) before HATU (10.7 mg, 0.028 mmol, 4 equiv) and DIEA (12.3 µL, 0.07 mmol, 10 equiv) were added to the solution of the cage **C** in 368 µL of DMF (9.0 mg, 0.005 mmol, 1 equiv). The reaction was left stirring overnight and the resulting reaction mixture was purified by RP-HPLC. $^{Tm}R_4C$ was obtained after RP-HPLC purification [Phenomenex Luna C18(2) 100A column, H_2O (0.1% TFA)/ CH_3CN (0.1% TFA) 85:15→55:45 (30 min)] with an overall yield of 13% (2.5 mg). R_t

11.9 min (Fig. S25). MS (ESI, H_2O) m/z: calcd for $C_{175}H_{249}N_{49}O_{13}$ $[M+4H]^{4+}$: 811.5, found: 812.4; calcd for $C_{179}H_{259}N_{49}O_{18}F_6$ $[M+10H+2TFA+H_2O]^{10+}$: 349.8, found: 349.7; calcd for $C_{183}H_{259}N_{49}O_{22}F_{12}$ $[M+8H+4TFA+H_2O]^{8+}$: 465.5, found: 465.3.

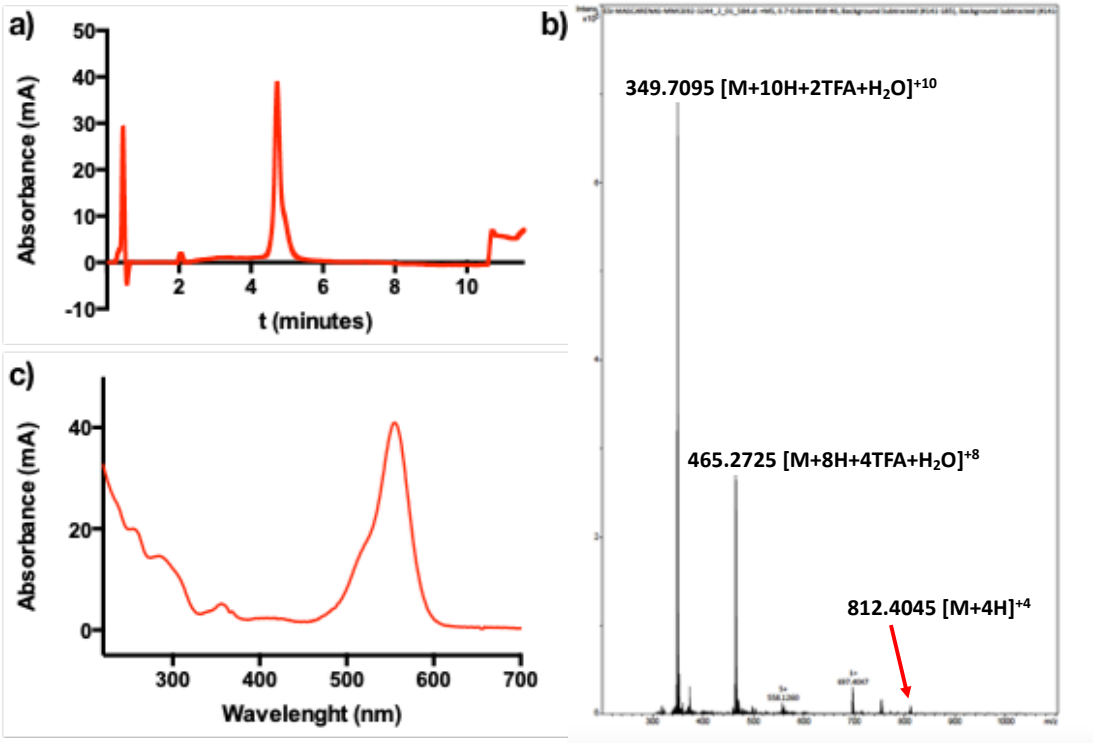

Figure S25. HPLC-MS spectra of $^{Tm}\boldsymbol{R_4}$**C**, a) chromatogram observed for λ=550 nm, b) ESI-MS spectrum corresponding to t = 4.73 minutes which corresponds to $^{Tm}\boldsymbol{R_4}$**C** and c) UV-Vis spectrum at 4.73 minutes corresponding to $^{Tm}\boldsymbol{R_4}$**C.**

4.2.4. Synthesis and characterization of peptide $^{Ac}\boldsymbol{R_4}$C

$^{Ac}\boldsymbol{R_4}$ was solved in 100 µL of DMF (10.3 mg, 0.011 mM) before HATU (4 mg, 0.011 mmol, 1 equiv) and DIEA (14.1 µL, 0.109 mmol, 10 equiv) were added to the solution of the cage **C** in 368 µL of DMF (20 mg, 0.011 mmol, 1 equiv). The reaction was left stirring overnight and the resulting reaction mixture was purified by RP-HPLC. $^{Ac}\boldsymbol{R_4}$**C** was obtained after RP-HPLC purification [Luna C18(2) 100A column, H_2O (0.1% TFA)/ CH_3CN (0.1% TFA) 85:15→55:45 (30 min)] with an overall yield of 10% (3.1 mg). R_t 10.5 min (Fig. S26). MS (ESI, H_2O) m/z: calcd for $C_{152}H_{227}N_{46}O_{15}F_9$ $[M+8H+3TFA]^{8+}$: 388.6, found: 387.5; calcd for $C_{154}H_{225}N_{46}O_{17}F_{12}$ $[M+5H+4TFA]^{5+}$: 644.0, found: 645.1.

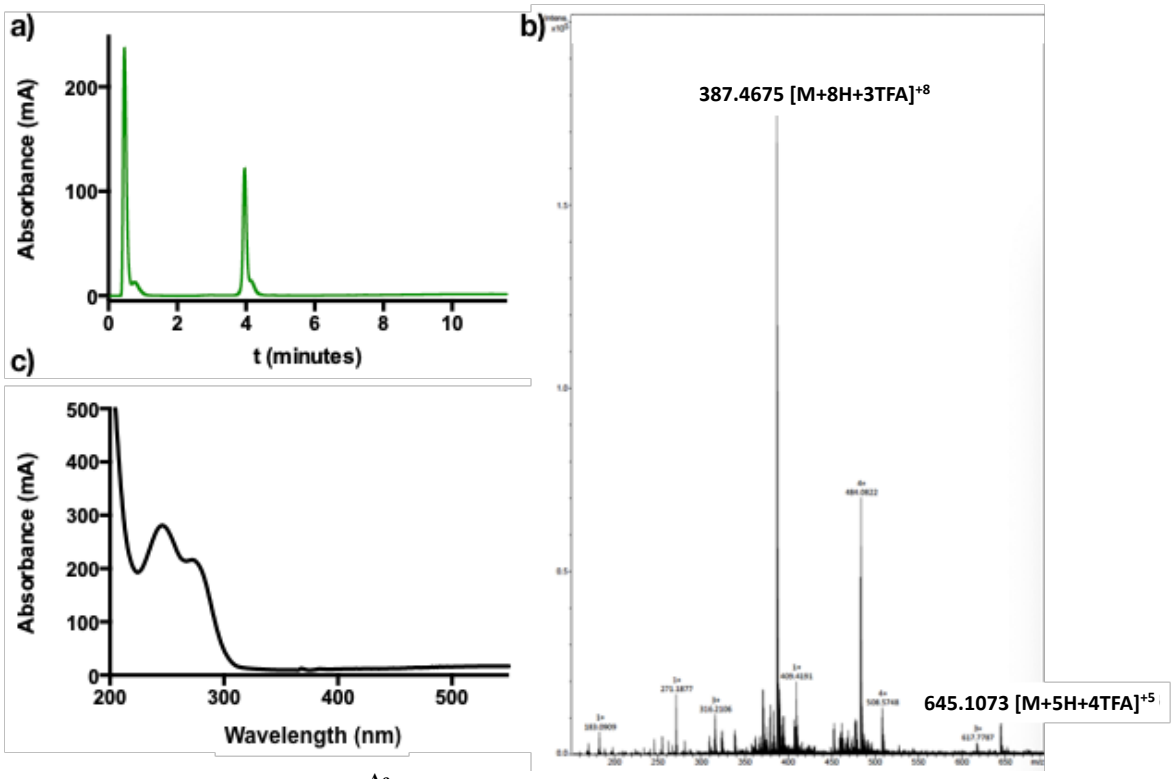

Figure S26. HPLC-MS spectra of $^{Ac}\boldsymbol{R}_4\mathbf{C}$, a) chromatogram observed for λ=222 nm, b) ESI-MS spectrum corresponding to t = 4.01 minutes which corresponds to $^{Ac}\boldsymbol{R}_4\mathbf{C}$ and c) UV-Vis spectrum at 4.01 minutes corresponding to $^{Ac}\boldsymbol{R}_4\mathbf{C}$.

5. References

1 J. Rodríguez, J. Mosquera, J. R. Couceiro, J. R. Nitschke, M. E. Vázquez and J. L. Mascareñas, *J. Am. Chem. Soc.*, 2017, **139**, 55–58.

2 J. Mosquera, S. Zarra and J. R. Nitschke, *Angew. Chem. Int. Ed.*, 2014, **53**, 1556–1559.